EFFECT OF MEDIUM MORPHOLOGY ON LAMINAR FLOW IN A CHANNEL PARTIALLY FILLED WITH A POROUS BED

Renato A. Silva[1]
Marcelo J.S. De-Lemos[2]
Departamento de Energia - IEME
Instituto Tecnológico de Aeronáutica - ITA
12228-900 - São José dos Campos - SP, Brazil
[1]renatoas@mec.ita.br
[2]delemos@ita.br

Abstract. *The behavior of laminar flow in a channel partially occupied with a porous bed was numerically analyzed. The Navier-Stokes equations were solved around the rods and within the region occupied by the fluid. Numerical results for a flow that past through a channel with cylindrical rods showed good agreement with those found in the literature. With this idea in mind, an investigation on the influence of a different rod shape, namely, square rod, on the velocity field and on the interaction at the interface between the clear flow and the bed was performed. This investigation showed that the medium morphology influences mass flux and mixing intensity between the unobstructed flow and the region filled with rods. This work also shows that, the higher the Darcy number of the bed, the higher the mass flux and the lower the mixing intensity between the two regions.*

Keywords*: hybrid media, porous bed, numerical solution, laminar flow, solids rods.*

1. Introduction

The study of a channel partially occupied with a porous bed, seen under a microscopic view in order to investigate the influence of the porous matrix morphology on the flow behavior, has not been completely documented in the available literature. And yet, the problem mentioned above is of great relevance to many areas of science and technology, which can benefit from such analysis. Some examples of applications are heat exchangers design and analysis of atmospheric boundary layer over forests and crops, to mention a few.

Many authors have investigated the porous medium influence in the flow behavior using several different approaches and modeling. In the works of Kuznetsov, 1996-2004, the flow in a channel partially occupied with a porous bed using two groups of equations, namely, one group for the porous medium and another for the clear medium, were investigated. In the mentioned works, the turbulence model was account only in the clear region. On the other hands, the flow in the porous media has been considered as laminar.

In the works of Kuwahara *et al.* 1994 and Nakayama *et al.* 1995, several porous media configurations partially filled by cylindrical, spherical and square rods was numerically simulated and showed that the bi-dimensional and the tri-dimensional models yield to very similar expressions for the permeability. In Kuwahara *et al.* 1998, the inner flow in an infinite porous medium formed by square rods with a spatially periodic arrangement using a Low-Reynolds turbulence model was investigated. A turbulent behavior of the flow was observed for Reynolds number of $Re_H > 10^4$ and in these conditions the extended model of Darcy-Forchheimer reproduces satisfactorily the phenomenon.

In Pedras and de-Lemos, 2001a-b, a macroscopic turbulence model, where a constant was introduced in the turbulence kinetic energy equation, was developed. The value of this constant was obtained through numerical simulations in a porous medium formed by cylindrical rods with a spatially periodic arrangement. In other related works, an extension of this adjustment for longitudinal and transversal elliptical rods was also performed, in Pedras and de-Lemos, 2001c-2003. In the works Silva and de-Lemos 2003a-b, numerical solutions for laminar and turbulent flow in a channel partially occupied with a porous bed were presented. Therein the shear stress jump at the interface proposed by by Ochoa-Tapia and Whitaker, 1995a-b are took into account.

In the investigation presented in Prinos *et al.* 2003, the authors analyzed the influence of the porosity and the Darcy number in an open channel containing a permeable layer considering a turbulent flow. The flow behavior over and into the porous region were analyzed by numerical simulation using a microscopic approach. In such work, the parameters of the medium and the statistical flow field on the permeable region were measured with a hot wire anemometer.

In the study presented in Breugem *et al.* 2004, the authors obtained results through Direct Numerical Simulation (DNS) for laminar flow in a channel occupied by a grid of cubes. Therein, simulations enable the direct evaluation of closure for the drag and the dispersion stress that are required to solve the Volume-Averaged Navier-Stokes equations for flow in porous media. In addition, according to Breugem *et al.* 2004, the model proposed in Ochoa-Tapia and Whitaker, 1995b had good agreement with the Direct Numerical Simulation. However, the value of the stress jump parameter is unknown a priori and this is one of the main disadvantages of such model. Also in Breugem *et al.* 2004, the results showed that the permeability depends not only on the porosity but also on the gradient in the volume-average velocity.

Motivated by the foregoing, the main objective of this work is to investigate the influence of the rods shape that composes the porous medium on the flow field, mass flux and in the interaction (mixing) of the flows above and below of the interface between the clear region and the region filled by an arrangement of rods.

2. Mathematical Model

2.1. Geometry and Governing Equations

The flow under consideration is schematically shown in Fig. 1*a* where a channel is partially occupied with solid rods localized at same height, h_c, (see Fig. 1*b*). A constant property fluid flows longitudinally from left to right.

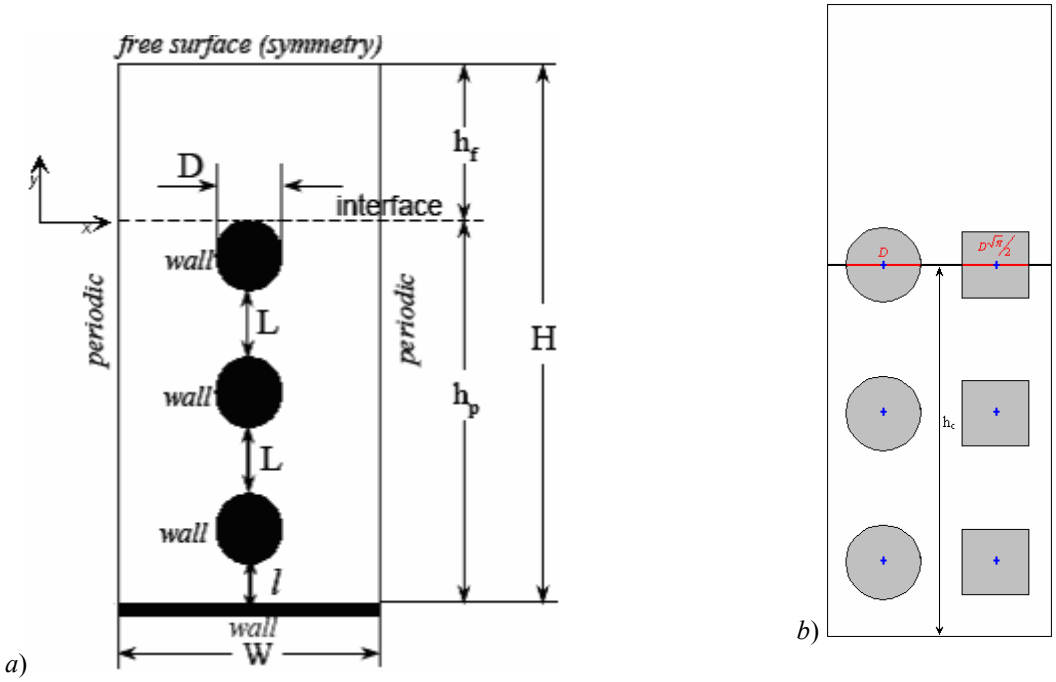

Figure 1: *a*) Geometry and boundary conditions, *b*) position of the rods.

The continuity equation is given by,

$$\nabla \cdot \mathbf{u} = 0 \tag{1}$$

The Navier-Stokes (NS) equation for an incompressible fluid with constant properties can be written as,

$$\rho(\mathbf{u}\nabla \cdot \mathbf{u}) = \rho\mathbf{g} - \nabla p + \mu\nabla^2\mathbf{u} \tag{2}$$

2.2. Numerical Procedure − Boundary Conditions

The equations (1) and (2) are solved by using a CFD commercial code. The computational domain, the coordinate system, the boundary conditions are showed in Fig. 1*a*. For channels containing cylindrical rods, it is applied a computational mesh consisted of quadrilateral (adjacent to the walls) and triangular (in the core flow region) elements (an example is showed in Fig. 2*a*). For channels containing square rods, the computational mesh applied consists of only quadrilateral elements and a mesh refinement is employed around the rods (see Fig. 2*b*).

In order to reach the developed flow, a spatial periodicity condition is applied to the upstream and downstream sides (given streamwise pressure gradient). At the free surface symmetry, condition is applied. In the lower wall and in the rods surfaces, a non-slip condition is applied.

The main characteristics of the numerical procedure used in CFD code, which is an elliptic iterative solver, are:

Discretization Schemes. Combination of bounded QUICK (at quadrilateral mesh elements) and Second Order Upwind (at triangular mesh elements) for u, v, Second Order for P (analogous to Second Order Upwind for convection terms above). PISO for velocity–pressure coupling.

Convergence. The periodic condition poses a difficulty in convergence, hence the large number of iterations. The problem may be considered quasi−elliptic (the boundary condition at the periodic faces is not fixed, rather it changes from iteration to iteration and progresses to its converged state very slowly). Numerical calculations were performed

utilizing a double precision and all normalized residuals were reduced to less than 10^{-8} before convergence was accepted.

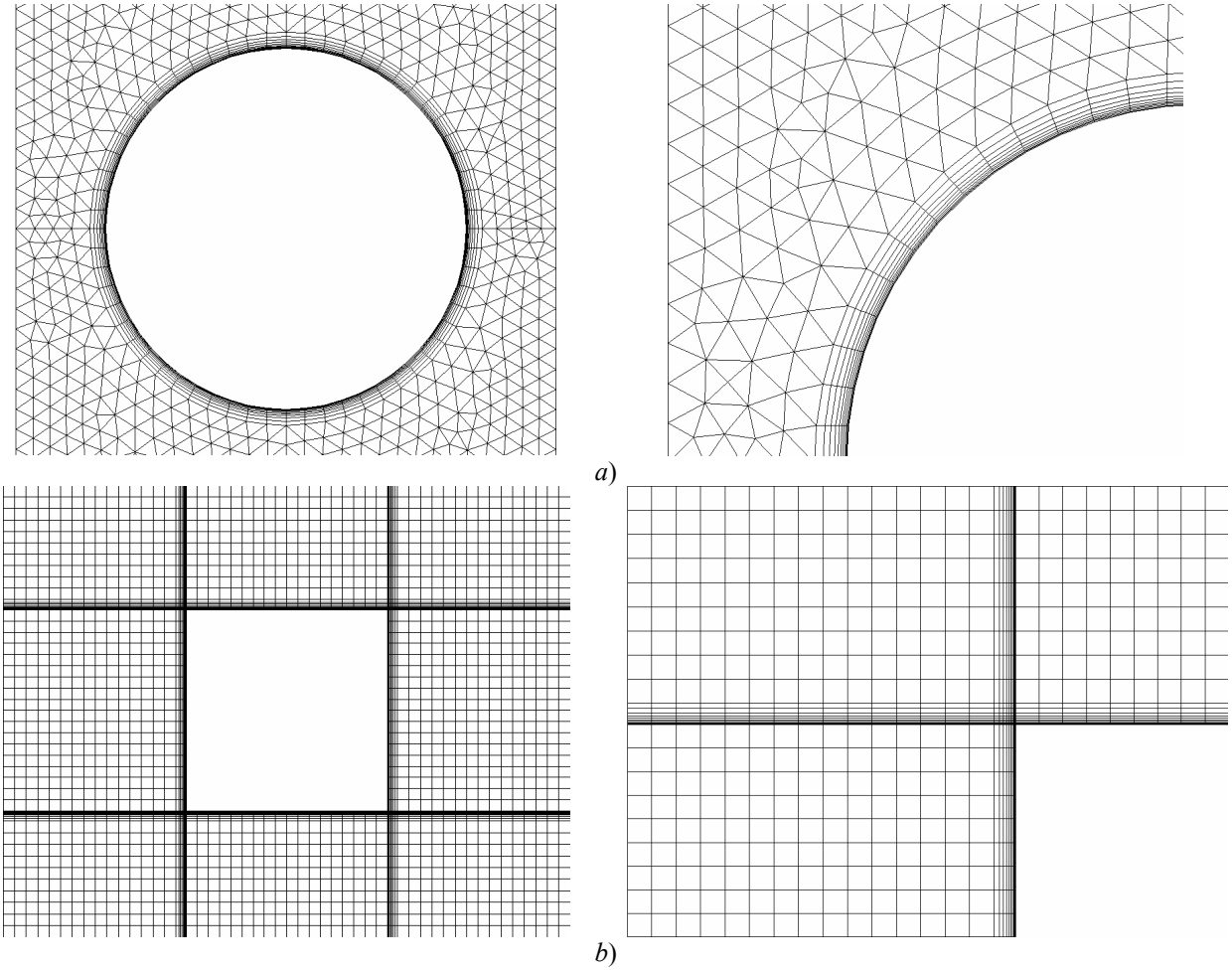

Figure 2: Computational mesh: *a*) triangular and rectangular elements, *b*) rectangular elements.

3. Results and conclusions

Table 1 shows geometrical data for the two configurations, ϕ=0.7144 (cases 150-30, 150-50 and 150-70) and ϕ=0.8286 (cases 250-30, 250-50 and 250-70), where the permeability, *K*, is estimated according to Bird *et al.* 1960. The Reynolds number, Re_f, is calculated considering an impermeable wall at the interface.

Table 1: Geometric characteristics – cylindrical rods.

Case	W [m]	H [m]	h_f [m]	h_p [m]	h_f/H	D [m]	Nº of Rods	ϕ	*K* [m^2]	Da	-dP/dx [N/m^3]	Re_f	Nº of Cells	Re_f	Nº of Cells
Cylindrical rods												Prinos *et al.* 2003		Present work	
150-30	0.015	0.0850	0.03	0.055	0.3529	0.01	3	0.7144	3.5700E-5	4.9412E-3	1.E-3	9.5558E0	10779	9.5600E0	9468
150-50		0.1050	0.05		0.4762					3.2381E-3		4.3055E1	11073	4.3081E1	11682
150-70		0.1250	0.07		0.5600					2.2848E-3		1.1611E2	10154	1.1679E2	13844
250-30	0.025	0.0850	0.03		0.3529	0.01	3	0.8286	4.1070E-4	5.6844E-2		1.0165E0	12025	1.0191E0	16024
250-50		0.1050	0.05		0.4762					3.7252E-2		4.4689E1	12853	4.4798E1	19348
250-70		0.1250	0.07		0.5600					2.6285E-2		1.1980E2	13815	1.1997E2	23584

Table 2 presents the hydrodynamic characteristics for a non-staggered arrangement of cylindrical rods, where $u_{int,po}$ is the punctual velocity at the intersection of the interface with the periodic plane. The average velocity at the interface, the average velocity in the clear region (above the rods) at the periodic plane and the average velocity in the porous region (below the interface) are, respectively, $u_{int,m}$, $u_{f,com}$ and $u_{p,com}$. Finally, u_D is the Darcy velocity, calculated

according to the Darcy law ($u_D = -\frac{K}{\mu}\frac{dP}{dx}$). Concerning Prinos *et al.* 2003, despite the fact that its results were obtained with a poorer mesh, a good agreement was observed between their results and the present computations.

Table 2: Hydrodynamics characteristics – cylindrical rods.

Case	$u_{int,po}$ [m/s]	$u_{int,m}$ [m/s]	$u_{f,com}$ [m/s]	u_D [m/s]	$u_{p,com}$ [m/s]
Cylindrical rods – Prinos *et al.* 2003					
150-30	2.9281E-5	2.2607E-5	3.2006E-4		5.7764E-6
150-50	6.3408E-5	3.6962E-5	8.6525E-4	3.5593E-5	6.1973E-6
150-70	8.7343E-5	5.0719E-5	1.6667E-3		6.6318E-6
250-30	7.2267E-5	4.4850E-5	3.4045E-4		9.9545E-6
250-50	1.1891E-4	7.1981E-5	8.9808E-4	4.0947E-4	1.1021E-5
250-70	1.6236E-4	9.7908E-5	1.7196E-3		1.1918E-5
Present results					
150-30	3.3680E-5	2.2305E-5	3.2020E-4		5.7675E-6
150-50	5.5420E-5	3.6673E-5	8.6576E-4	3.5593E-5	6.1906E-6
150-70	7.7015E-5	5.1316E-5	1.6765E-3		6.5938E-6
250-30	6.4243E-5	4.4809E-5	3.4132E-4		9.9706E-6
250-50	1.0256E-4	7.1561E-5	9.0027E-4	4.0947E-4	1.1021E-5
250-70	1.3873E-4	9.7642E-5	1.7221E-3		1.1880E-5

Table 3 shows the geometrical characteristics of two configurations, ϕ=0.7114 (cases 150-30, 150-50 and 150-70) and ϕ=0.8268 (cases 250-30, 250-50 and 250-70), for a non-staggered arrangement of square rods; where the Re_f value, are calculated considering an impermeable wall at the interface. The permeability, *K*, is numerically calculated by solving the flow equations inside the elementary Control Volume with an area of $\left[H_{CV} = \left(\frac{D\sqrt{\pi}}{2} + 2l\right)\right] \times W$, where *l*=L/2, for the Darcy regime (creeping flow, $\mathrm{Re}_{H_{CV}} < 1$). This elementary control volume is represented by an infinite long porous medium, with a symmetrical boundary condition at the north and south faces and a periodical condition at the east and west faces. Table 3, also, presents the permeability of a channel with cylindrical rods where *K* was calculated using the procedures already described above, note that the calculated permeability for cylindrical rods (using the Darcy law) is higher than the permeability of the square rod case.

Table 3: Geometric characteristics – square rods.

Case	W [m]	H [m]	h_f [m]	h_p [m]	h_f/H	D [m]	Nº of Rods	ϕ	*K* [m^2]	Da	-dP/dx [N/m^3]	Re_f	Nº of Cells	*K* [m^2]	Da
Square rods														Cylindrical rods	
150-30		0.0850	0.0306		0.3600					8.8449E-4		9.6097E0	10212		9.0668E-4
150-50	0.015	0.1050	0.0506		0.4819	0.01	3	0.7114	6.3902E-6	5.7961E-4		4.3024E1	12132	6.5508E-6	5.9418E-4
150-70		0.1250	0.0706	0.0544	0.5648					4.0897E-4	1.E-3	1.1705E2	14052		4.1925E-4
250-30		0.0850	0.0306		0.3600					1.2101E-3		1.0126E1	14872		1.3301E-3
250-50	0.025	0.1050	0.0506		0.4819	0.01	3	0.8268	8.7431E-6	7.9302E-4		4.4627E1	17592	9.6097E-6	8.7163E-4
250-70		0.1250	0.0706		0.5648					5.5956E-4		1.1980E2	20312		6.1502E-4

Table 4 presents a comparison between the hydrodynamic characteristics of cylindrical and square rods, all in a non-staggered arrangement. Note that the Darcy velocity, u_D, for square rods, is obtained through Darcy law and the center of the square rods is located in the same position as the cylindrical case. Also, observe that the velocities (in Tab. 4) for cylindrical rods are higher than the velocities for square rods.

Table 4: Hydrodynamics characteristics.

Case	$u_{int,po}$ [m/s]	$u_{int,m}$ [m/s]	$u_{f,com}$ [m/s]	u_D [m/s]	$u_{p,com}$ [m/s]
Cylindrical rods - Present results					
150-30	3.3680E-5	2.2305E-5	3.2020E-4		5.7675E-6
150-50	5.5420E-5	3.6673E-5	8.6576E-4	3.5593E-5	6.1906E-6
150-70	7.7015E-5	5.1316E-5	1.6765E-3		6.5938E-6
250-30	6.4243E-5	4.4809E-5	3.4132E-4		9.9706E-6
250-50	1.0256E-4	7.1561E-5	9.0027E-4	4.0947E-4	1.1021E-5
250-70	1.3873E-4	9.7642E-5	1.7221E-3		1.1880E-5
Square rods					
150-30	1.7400E-5	8.3911E-6	3.1586E-4		5.0935E-6
150-50	2.8624E-5	1.3740E-5	8.5842E-4	6.3711E-6	5.1560E-6
150-70	3.9775E-5	1.9046E-5	1.6665E-3		5.2164E-6
250-30	4.8250E-5	3.0928E-5	3.3285E-4		7.9044E-6
250-50	7.7630E-5	4.9653E-5	8.8673E-4	8.7169E-6	8.1926E-6
250-70	1.0593E-4	6.7663E-5	1.7058E-3		8.3694E-6

In Fig. 3, it can be seen a comparison between the velocity fields presented by Prinos *et al.* 2003 and the present results for two values of Da. The velocity was normalized by the punctual velocity at the intersections of the interface with the periodic plane in order to indicate the interaction between the flow above and below the rods. The velocity field shows an increase of *momentum* exchange with higher Da numbers. (Note that the solution domain was graphically repeated in the streamwise direction for clarity reasons and those white areas in the region of the rods wake indicate negative streamwise velocity, i.e., recirculation). It is observed that there is a good accordance between the results.

Figure 4 presents the velocity field of the square rods case for two Da values. It is noticed an increase of the *momentum* exchange for higher Da numbers, and that the white areas indicate recirculation. Contours of u/uint,po indicate that mixing (interaction) increases with higher Da number, resulting in a decrease of the maximum u/uint,po from 26 to 17.3. Also, velocities below the interface increase with higher Da number.

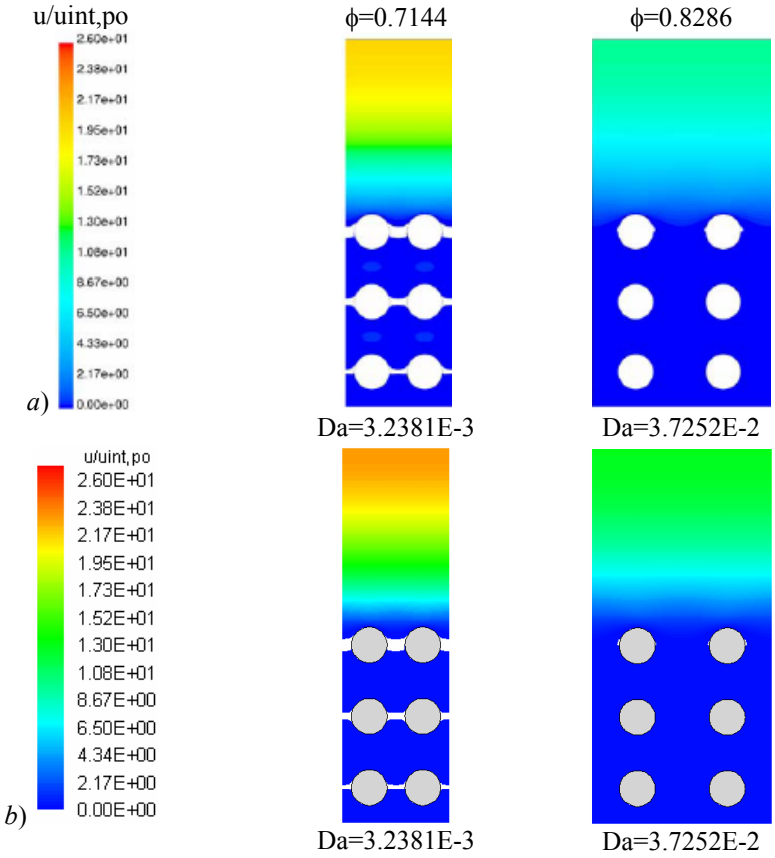

Figure 3: Velocity fields for: *a*) cylindrical rods case - Prinos *et al.* 2003, *b*) cylindrical rods case - Present Results.

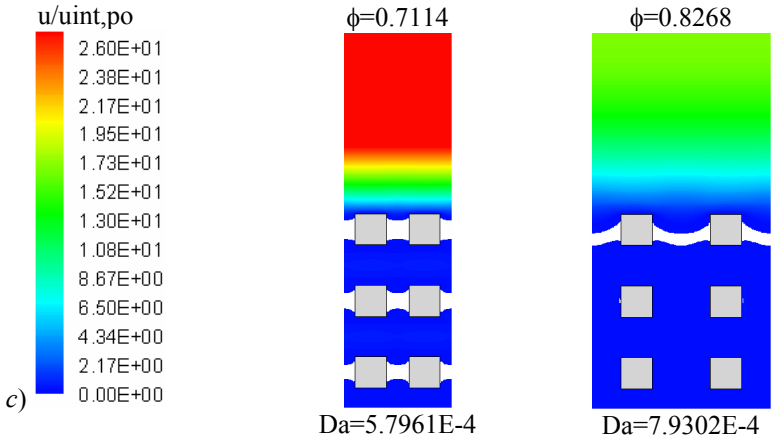

Figure 4: Velocity fields for square rods case.

Figure 5*a* shows a comparison between the obtained velocity profiles and the result of Prinos *et al.* 2003 for a channel containing cylindrical rods with h/H=0.3529 and two Darcy numbers. Note that, besides the good agreement between the results, the mass flow rate increases with higher Darcy numbers, $Da = \frac{K}{H^2}$, where K is the permeability of the porous medium, which can be physically understood as the difficulty of the fluid to go thorough the imposed drag caused by the shape and the geometrical arrangement of the porous matrix.

In Fig. 5*b*, it is investigated the effect of the square rods in the velocity profile, for h/H=0.3600 and two Darcy numbers. Note that the mass flow rate as in the region containing the rods, as in the clear region, is lower than the mass flow rate in a channel with cylindrical rods (see Tab. 4).

Figure 5*c* shows a comparison between the obtained velocity profiles and the result of Prinos *et al.* 2003 for a channel containing cylindrical rods with h/H=0.4762 and two Darcy numbers. It was found a good agreement between the results. Also, the mass flow rate increases with higher Darcy numbers.

In Fig. 5*d*, it is analyzed the influence of the square rods in the flow behavior, for h/H=0.4819 and two Darcy numbers. It is noted an increase of the mass flow rate with higher Darcy numbers along all the cross section of the channel, indicating an increase in the momentum exchange between the regions above and below the interface.

According to Fig. 5*e*, a good agreement is found between the obtained velocity profiles and the results of Prinos *et al.* 2003 for a channel containing cylindrical rods with h/H=0.5600 and two Darcy numbers. Note that there is an increase of the flow mass rate as in the region with rods as in the clear region with higher Darcy numbers.

The effect of the square rods in the flow behavior with h/H=0.5648 and two Darcy numbers is observed in Fig. 5*f*. Observe that there is an increase of the flow mass rate with higher Darcy numbers.

4. Conclusions

The flow in a channel containing a porous bed composed by a non-staggered arrangement of cylindrical, square rods was investigated for different porosity and Darcy number values. According to the obtained results, it was observed the following:

i) for cylindrical rods was found a good accordance between present results and the data showed in Prinos *et al.* 2003;

ii) the increase in the resistance imposed to the flow (decrease Da number) due to the shape and the arrangement of the rod, results in a decrease of the flow rate of the channel;

iii) the *momentum* exchange at the interface increases with the Darcy number, meaning that there is an increase in the interaction between the flow over and under the interface region.

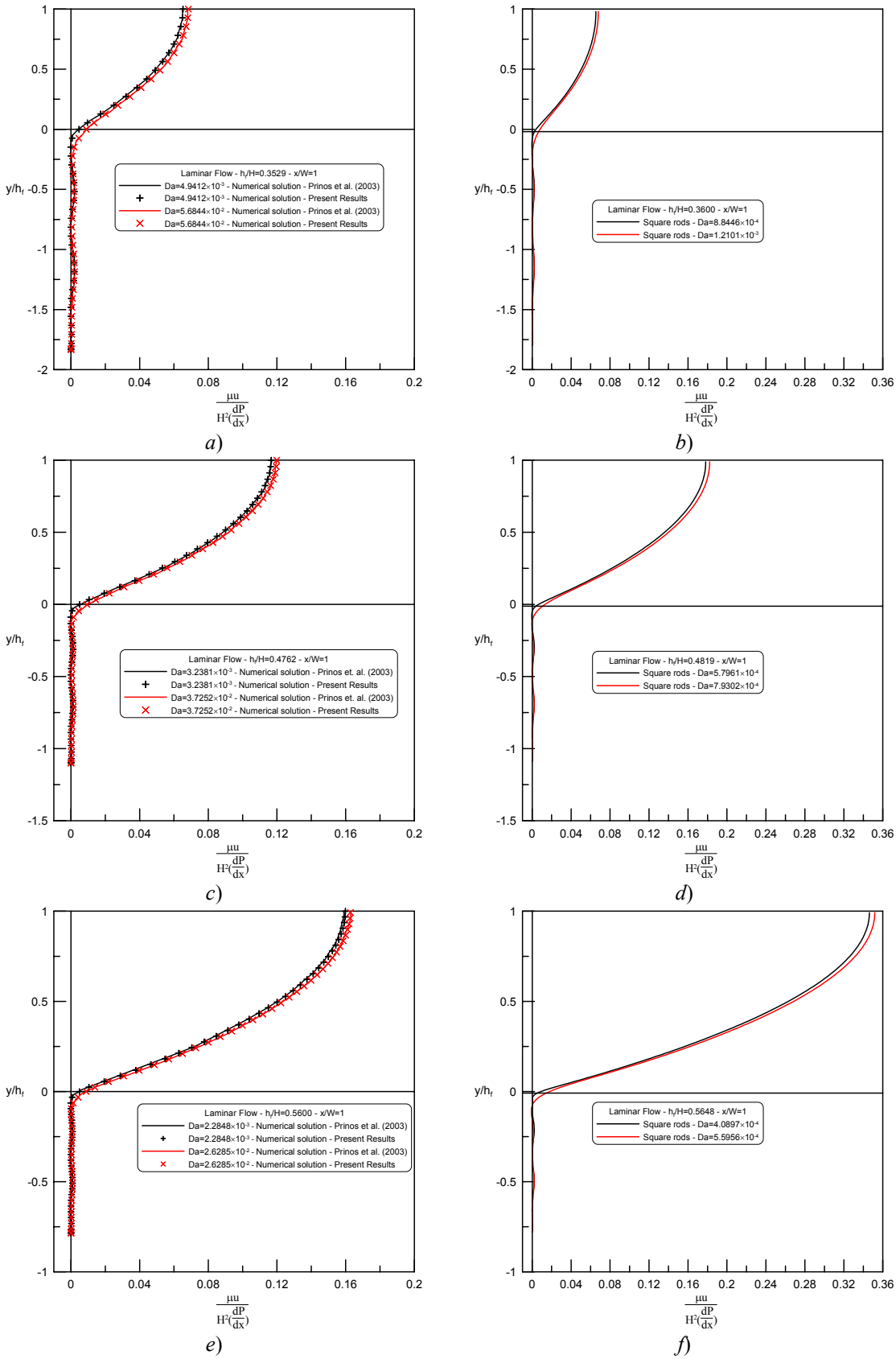

Figure 5: Effect of Darcy number in the velocity profile, *a*) channel with cylindrical rods, *b*) channel with square rods.

5. Acknowledgments

The authors would like to express their gratitude to CNPq and FAPESP, Brazil, for the invaluable financial support during the course of this research.

6. References

Bird, R.B., Steward, W.E. and Lighfoot, E.N., 1960, "Transport Phenomena", Wiley, New York.

Breugem, W.P., Boersma, B.J. and Uittenbogaard, R.E., 2004, "Direct Numerical Simulations of Plane Channel Flow over a 3D Cartesian Grid of Cubes", in: Proc. of International Conference on Porous Media and Applications, pp. 27-35.

Kuwahara, F., Nakayama, A. and Koyama, H., 1994, "Numerical Modeling of Heat and Fluid Flow in a Porous Medium", in: Proc. of Int. Heat Transfer Conf., Vol. 5, pp. 309-314.

Kuwahara, F., Kameyama, Y., Yamashita, S. and Nakayama, A., 1998, "Numerical Modeling of Turbulent Flow in Porous Media using a Spatially Periodic Array", J. Porous Media, Vol. 1, nº 1, pp. 47-55.

Kuznetsov, A.V., 1996, "Analytical Investigation of the Fluid Flow in the Interface Region between a Porous Medium and a Clear Fluid in Channels Partially Filled with a Porous Medium", Applied Scientific Research, Vol. 56, pp. 53-67.

Kuznetsov, A.V., 1997, "Influence of the Stress Jump Condition at the Porous-Medium/Clear-Fluid Interface on a Flow at a Porous Wall", International Communication Heat Mass Transfer, Vol. 24, nº 3, pp. 401-410.

Kuznetsov, A.V., 1998, "Analytical Investigation of Couette Flow in a Composite Channel Partially Filled with a Porous Medium and Partially with a Clear Fluid", International Journal Heat Mass Transfer, Vol. 41, nº 16, pp. 2556-2560.

Kuznetsov, A.V., 1999, "Fluid Mechanics and Heat Transfer in the Interface Region between a Porous Medium and Fluid Layer: a Boundary Layer Solution", Journal of Porous Media, Vol. 2, nº 3, pp. 309-321.

Kuznetsov, A.V., Cheng, L. and Xiong, M., 2002, "Effects of Thermal Dispersion and Turbulence in Forced Convection in a Composite Parallel-Plate Channel: Investigation of Constant Wall Heat Flux and Constant Wall Temperature", Vol. 42, pp. 365-383.

Kuznetsov, A.V. and Xiong, M., 2003, "Development of an Engineering Approach to Computations of Turbulent Flows in Composite Porous/Fluid Domains", International Journal of Thermal Sciences, Vol. 42, pp. 913-919.

Kuznetsov, A.V. and Backer, S.M., 2004, "Effect of the Interface Roughness on Turbulent Convective Heat Transfer in a Composite Porous/Fluid Duct", Int. Comm. Heat Mass Transfer, Vol. 31, nº 1, pp. 11-20.

Nakayama, A., Kuwahara, F., Kawamura, Y. and Koyama, H., 1995, "Three-Dimensional Numerical Simulation of Flow through a Microscopic Porous Structure", in: Proc. ASME/JSME Thermal Engineering Conf., Vol. 3, pp. 313-318.

Ochoa-Tapia, J.A. and Whitaker, S., 1995a, "Momentum Transfer at the Boundary between a Porous Medium and a Homogeneous Fluid – I", International Journal of Heat and Mass Transfer, Vol. 38, nº 14, pp. 2635-2646.

Ochoa-Tapia, J.A. and Whitaker, S., 1995b, "Momentum Transfer at the Boundary between a Porous Medium and a Homogeneous Fluid – II", International Journal of Heat and Mass Transfer, Vol. 38, nº 14, pp. 2647-2655.

Pedras, M.H.J. and de-Lemos, M.J.S., 2001a, "Macroscopic Turbulence Modeling for Incompressible Flow through Undeformable Porous Media", Intern. J. Heat and Mass Transfer, Vol 44, nº 6, pp. 1081-1093.

Pedras, M.H.J. and de-Lemos, M.J.S., 2001b, "Simulation of Turbulent Flow in Porous Media using a Spatially Periodic Array and a Low Re Two-Equation Closure", Numerical Heat Transfer - Part A – Applications, Vol. 39, nº 1, pp. 35-59.

Pedras, M.H.J. and de-Lemos, M.J.S., 2001c, "On the Mathematical Description and Simulation of Turbulent Flow in a Porous Medium Formed by an Array of Elliptic Rods", Journal of Fluids Engineering, Vol. 123, nº 4, pp. 941-947.

Pedras, M.H.J. and de-Lemos, M.J.S., 2003, "Computation of Turbulent Flow in Porous Media using a Low-Reynolds k-ε Model an Infinite Array of Spatially Periodic Elliptic Rods", Numerical Heat Transfer – Part A – Applications, Vol. 43, nº 6, pp. 585-602.

Prinos, P., Sofialidis, D. and Keramaris, E., 2003, "Turbulent Flow over and within a Porous Bed", Journal of Hydraulic Engineering, Vol. 129, nº 9, pp. 720-733.

Silva, R.A. and de-Lemos, M.J.S., 2003a, "Turbulent Flow in a Channel Occupied by a Porous Layer Considering the Stress Jump at the Interface", Inter. Journal of Heat and Mass Transfer, Vol. 46, pp. 5113-5121.

Silva, R.A. and de-Lemos, M.J.S., 2003b, "Numerical Analysis of the Stress Jump Interface Condition for Laminar Flow over a Porous Layer", Numerical Heat Transfer - Part A – Applications, Vol. 43, pp. 603-617.